MATHEMATICAL MODELING AND COMPUTING, Vol. 12, No. 2, pp. 363–374 (2025)

Magnetohydrodynamics flow of hybrid nanofluid over a heated thin needle

Ilias M. R.[1,3], Awang N.[2], Fazri N. N.[2], Rosmadi S. A. A.[2], Salleh S. N. A.[4], Nazar R. M.[3]

[1] *School of Computing, Informatics and Mathematics, University Teknologi MARA, 40450 Shah Alam, Selangor, Malaysia*
[2] *Mathematical Sciences Studies, College of Computing, Informatics and Mathematics, University Teknologi MARA Negeri Sembilan Branch, Seremban Campus, 70300 Seremban, Negeri Sembilan, Malaysia*
[3] *Department of Mathematical Sciences, Faculty of Science and Technology, University Kebangsaan Malaysia, Bangi 43600, Malaysia*
[4] *Mathematical Sciences Studies, College of Computing, Informatics and Mathematics, University Teknologi MARA Kedah Branch, 08400 Merbok, Kedah, Malaysia*

(Received 18 December 2024; Revised 15 April 2025; Accepted 17 April 2025)

Suspending nanoparticles in the base fluid can effectively improve the thermal conductivity of a fluid. Therefore, this study focuses on a steady two-dimensional laminar forced convection boundary layer flow along a horizontal thin heated needle immersed in a hybrid nanofluid with convective boundary condition. Copper and aluminium oxide nanoparticles with water as based fluid were selected for this study. The governing partial differential equations are transformed into nonlinear ordinary differential equations by using an appropriate similarity transformation. These equations are then solved numerically using bvp4c package in MATLAB software. The effect of the involved parameters of interest, including nanoparticles volume fraction, needle thickness, velocity ratio, dimensionless slip length, interaction of magnetic field and convective boundary condition on the velocity and temperature profiles, as well as the skin friction coefficient and the local Nusselt number are illustrated through graphs and tables. The result shows that as the nanoparticles volume fraction and dimensionless slip length parameter increase, the velocity profile increases. On the other hand, the temperature increases when the parameters of needle thickness, dimensionless slip length, interaction of magnetic field, volume fraction of nanoparticles, velocity ratio parameter and convective boundary condition increase. Overall, as the parameters increase Cu-Al_2O_3/water have higher values of skin friction and Nusselt number compared to water. The applications of this investigation can be applied in the field of biomedical engineering where heated needles play a crucial role in medical treatments such as thermal ablation, drug delivery, and minimally invasive surgeries.

Keywords: *hybrid nanofluid; horizontal thin needle; magnetohydrodynamics; convective boundary condition.*

2010 MSC: 35B40, 76D05, 35Q30, 76D10, 76S05 **DOI:** 10.23939/mmc2025.02.363

1. Introduction

In the field of industrial and technological applications, nanofluids play an important role due to their superior physical, chemical and thermal performance. The purpose of using nanofluids is to increase the thermal conductivity of the fluid. One of the techniques, to increase the effective thermal conductivity of this mass transfer fluid, is to add nanoparticles in the base fluid. Choi [1] was the first to study heat transfer in nanofluids. According to Choi [1] and Eastman et al. [2], a nanofluid is a fluid composed of nanoparticles dispersed in a base fluid. Besides that, the heat transfer performance can be more increased by using hybrid nanofluid. Hybrid nanofluid is a relation between two or more

This work was funded by Ph.D. Graduate MyRA Research Grant (600-RMC/GPM LPHD 5/3 (158/2021)) from University Teknologi MARA.

types of nanoparticles that hang in a base fluid and a combination of favorable physical and chemical properties that will make it more stable and boost thermophysical properties [3].

Research has been done to examine the effects of nanofluid through a variety of geometries, including the thin needle. Nanoparticles in nanofluids have been found to alter the boundary layer flow around thin needles. There are a few studies that have been done considering a thin needle [4, 5]. Waini et al. [6] studied the dynamics of hybrid nanofluid flow and the heat transmission across a thin needle by integrating the specified surface heat flux as a parameter in the research. The result of the research indicates improvement in the heat transfer properties and the coefficient of friction drag due to a decline in the needle size and volume fraction of nanoparticles. Hamid [7] conducted research to study the behaviour of nanofluid around a thin needle along with the influence from the Joule heating and viscous dissipation effects. The investigation on the flow of a hybrid nanofluid past a moving slender needle is examined by Aladdin et al. [8] considering the impact of magnetic field and slip. Another study on a hybrid nanofluid flow past a thin needle is done by Prashar et al. [9]. They found from their analysis that adding nanoparticles to conventional fluids can greatly improve the heat transport in the boundary layer. Singh et al. [10] investigated the flow of nanofluid by considering the physical processes like the transmission of heat and mass transfer to study the effect of the mentioned processes on the boundary conditions of a needle. Based on the research, it is discovered that as the dimension-independent needle increases in size, it is observed that there is the decline in the shearing force and transmission rate. Very recently, Ali et al. [11] extended the discussion on the behaviour of the boundary layer along a moving thin needle by incorporating the influence of magnetofluid dynamics and combined convection. The research concludes that increase in the magnetofluid dynamics increases the temperature while causing a decline in the velocity profiles.

Heat flux and constant surface temperature are two temperature conditions that are frequently used in heat transfer studies. In some situations, the amount of heat conveyed to the surface varies depending upon its temperature; that is typically the situation with heat exchangers. Convective boundary conditions should therefore be considered. Waini et al. [12] are motivated to explore the behavior of heat transfer and hybrid nanofluid flow beyond a permeable stretching/shrinking surface involving a convective boundary condition after analyzing earlier studies. In light of its usefulness in a wide variety of areas, such as paper manufacturing, glass blowing, and artificial fiber creation, the varied hybrid nanofluids boundary layer motion over the stretchable/shrinking wedge has attracted substantial attention in recent decades [13]. A thicker thermal boundary layer would suggest a less rapid rate of heat transfer within the fluid [14]. In this study, Jusoh et al. [15] emphasized the effects of viscous dissipation and the convective boundary condition upon the heat transfer within the Ag-Cu hybrid nanofluid. Convective boundary conditions are another aspect of boundary layer flow study that the author mentioned. Periodically, it is also known as the Robin condition. It can be described physically as an equal distribution of heat convection and conduction at the surface. The interplay between axial wall conduction and the thermal boundary layer development in the heated fluid influences heat exchange performance. Procedures involving high temperatures also entail convective heat transfers [15].

The magnetohydrodynamics (MHD) is a field that comprehends the magnetic properties of fluids exhibiting electrical conductivity like salt water, plasmas and electrolytes. It plays a vital role in various devices such as electrostatic filters, generators, power pumps, and heat exchangers [7]. Within fluid mechanics, the course of MHD explores the processes that occurs when magnetic field is implemented to a fluid with electrical conductivity properties. In electrically conductive fluids, MHD flow additionally influences the control of heat transmission rates at the surface, enabling the a desired cooling effect to be acquired [16]. In recent times, the MHD interface-layer stream of nanofluid has gained considerable attention across the domains of industry, science, and engineering [17]. Researchers have explored the influence of MHD on ferrofluids within a semi-circular annulus, revealing enhanced heat transfer rates associated with increased Rayleigh numbers and solid volume fractions [16]. Reference [8] investigated the behaviour of the boundary layer of two-dimensional axisymmetric incompressible MHD flow of

TiO_2-$C_2H_6O_2$ nanofluid on a vertical thin needle by incorporating the joule heating. In this research [8], a new analysis of the behaviour of the TiO_2-$C_2H_6O_2$ nanofluid flow of nanofluids and heat transfer impacted by MHD, joule heating, mixed convection, and nanoparticle aggregation is presented. The velocity profile shows an upward trend with increasing values of the mixed convection and velocity ratio parameters, and a downward trend with increasing values of the MHD and needle thickness parameters. The temperature profile shows a positive correlation with the nanoparticle volume fraction, MHD, needle thickness, velocity ratio, and Eckert number parameter. This implies that the temperature profile increases along with these parameters. In 2017, Sulochana et al. [18] addressed the movement of a tinny needle on the surface that constantly travels and parallels the free stream. The authors find that several solutions exist if both the needle and the free stream moved in the reverse direction. Also, Souayeh et al. [19] examined Casson fluid on a thin needle horizontally and concluded that in the case of moving a small needle, the hydrodynamic boundary layer is increased but shrinks in a fixed needle.

Motivated by the discussion above, this research extends the work by [8] by studying boundary layer flow and heat transfer over a moving horizontal slender needle in presence of convective boundary condition. The governing equations is simplified by using similarity transformations and solve by using bvp4c method in MATLAB software. The obtained numerical results are presented via graphs and tables.

2. Mathematical modeling

Examine the problem of a two-dimensional steady boundary layer of a hybrid nanofluid, composed of two distinct nanoparticles (Cu and Al_2O_3) in a water base fluid, flowing over a slender horizontal needle, as illustrated in Figure 1. The hybrid nanofluid is considered to be in thermal equilibrium with a slip boundary condition. We assume that the bottom surface of the needle is heated by convection from a hot fluid at a temperature T_f with T_∞ as the ambient temperature, resulting in a heat transfer coefficient h_f, along with an applied magnetic field. Additionally, the needle moves at a constant velocity U_w, either in the same direction as or opposite to the free stream velocity U_∞.

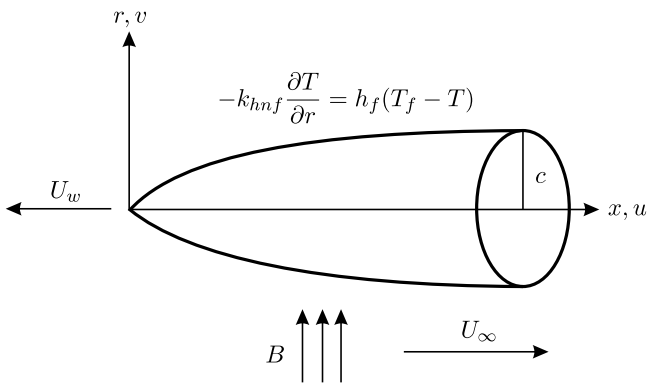

Fig. 1. Model of physical geometry.

Based on the model proposed by [8], the governing equations for our problem are as follows:

$$\frac{\partial(ru)}{\partial x} + \frac{\partial(rv)}{\partial r} = 0, \tag{1}$$

$$u\frac{\partial u}{\partial x} + v\frac{\partial u}{\partial r} = \frac{\mu_{hnf}}{\rho_{hnf}}\frac{1}{r}\frac{\partial}{\partial r}\left(r\frac{\partial u}{\partial r}\right) + \frac{\sigma B_0^2 u}{\rho_{hnf}}, \tag{2}$$

$$u\frac{\partial T}{\partial x} + v\frac{\partial T}{\partial r} = \frac{k_{hnf}}{(\rho C_p)_{hnf}}\frac{1}{r}\frac{\partial}{\partial r}\left(r\frac{\partial T}{\partial r}\right), \tag{3}$$

with assumptions of convective boundary conditions

$$u = U_w + Lu_r, \quad v = 0, \quad -k_{hnf}\frac{\partial T}{\partial r} = h_f(T_f - T) \quad \text{at} \quad r = R(x),$$
$$u \to U_\infty, \quad T \to T_\infty \quad \text{as} \quad r \to \infty. \tag{4}$$

Here u and v are the component of velocity for x axis and r axis, respectively, μ is the dynamic viscosity, ρ is the density, σ is the electrical conductivity, $B_0 = B\sqrt{x}$ is the uniform magnetic field imposed along the r axis, T is the hybrid nanofluid temperature in the flow, k is the thermal conductivity, C_p is the specific thermal at uniform pressure and $L = L_0 x/r$ is the slip length. Note that the subscript of hnf represents hybrid nanofluids.

The thermophysical properties of the regular fluid and nanoparticles are listed in Table 1. Additional details on applied relations for physical properties of hybrid nanoliquid can be found in the work of Devi and Devi [20]. Combining Al_2O_3 nanoparticles with 0.05 volume of Cu/water leads to the formation of a hybrid nanofluid. It is noteworthy that Cu nanoparticles, with a solid fraction of 0.05 ($\varphi 1 = 0.05$), are consistently added to the water throughout most of the analysis. Additionally, Al_2O_3 ($\varphi 2$) is incorporated to create a Cu-Al_2O_3/water.

Table 1. Thermophysical properties of the base fluid and nanoparticles [21].

Thermophysical properties	k (W/mK)	C_p (J/kg)K	ρ (kg/m^3)
Copper (Cu)	400	385	893
Alumina Oxide (Al_2O_3)	40	765	3970
Water	0.613	4179	997.1

We define a stream function ψ, such that $u = \psi_r/r$ and $v = -\psi_x/r$. The independent variables x and r in the aforementioned PDEs need to be eliminated. Therefore, we utilize similarity transformations to convert them into an ordinary differential equation with η as the new independent variable. The resulting similarities are as follows [8]:

$$\eta = \frac{U\,r^2}{\nu_f x}, \quad \psi = \nu_f\, x\, f(\eta), \quad \theta(\eta) = \frac{T - T_\infty}{T_f - T_\infty}, \tag{5}$$

where η is the similarity variable, $U = U_w + U_\infty$ is the combined velocity between the needle and the free stream flow, $\nu_f = \mu_f/\rho_f$ is the kinematic viscosity of the fluid, θ is the dimensionless temperature profile and the subscript of f refers to fluid.

By employing the stream function, Eq. (1) is satisfied identically. Assuming $\eta = c$ (as referenced by the needle size), Equation (5) defines the size and shape of the needle, with its surface described by

$$R(x) = \left(\frac{\nu_f c x}{U}\right)^{1/2}. \tag{6}$$

Replacing Eq. (5) into Eqs. (2)–(3) reduces this to the following nonlinear ordinary differential equations:

$$2\frac{\mu_{hnf}/\mu_f}{\rho_{hnf}/\rho_f}\left[\eta f'''(\eta) + f''(\eta)\right] - M f'(\eta) + f(\eta) f''(\eta) = 0, \tag{7}$$

$$\frac{2}{\Pr}\frac{k_{hnf}/k_f}{(\rho\, C_p)_{hnf}/(\rho\, C_p)_f}\left[\eta\,\theta''(\eta) + \theta'(\eta)\right] + f(\eta)\theta'(\eta) = 0, \tag{8}$$

together with the boundary conditions:

$$f(c) = \frac{1}{2}\varepsilon\, c + 2\sigma c\, f''(c), \quad f'(c) = \frac{1}{2}\varepsilon + 2\sigma\, f''(c), \quad \theta'(c) = -\frac{k_f}{k_{hnf}}\mathrm{Bi}\big[1 - \theta(c)\big],$$

$$f'(\eta) \to \frac{1}{2}(1 - \varepsilon), \quad \theta(\eta) \to 0 \quad \text{as} \quad \eta \to \infty. \tag{9}$$

In Eqs. (7)–(9), $M = \sigma B_0^2/2\rho_{hnf}U$ is the magnetic field parameter, $\Pr = \nu_f/\alpha_f$ is the Prandtl number, $\varepsilon = U_w/U$ is the velocity ratio variable, $\sigma = UL_0/\nu_f$ is the slip parameter and $\mathrm{Bi}_x = h_f v_f x/2Urk_f$ is the Biot number or convective parameter. However for energy equation to have a similarity solution, the parameter Bi must be a constant and not a function of x. This condition can only be satisfied if the heat transfer coefficient, h_f is proportional to x^{-1}. Hence, we assume $h_f = dx^{-1}$, where d is a constant. Therefore, $\mathrm{Bi} = dv_f/2Urk_f$.

The important physical quantities in this work are C_f and Nu_x which can be represented as [8]:

$$C_f = \frac{\mu_{hnf}}{\rho_f U^2}\left(\frac{\partial u}{\partial r}\right)_{r=c}, \quad \mathrm{Nu}_x = -\frac{x k_{hnf}}{k_f(T_f - T_\infty)}\left(\frac{\partial T}{\partial r}\right)_{r=c}. \tag{10}$$

Solving Eq. (10) in conjunction with Eq. (5) produces the following:

$$C_f \mathrm{Re}_x^{1/2} = \frac{4}{(1-\varphi)^{2.5}} c^{1/2} f''(c), \quad \mathrm{Nu}_x \mathrm{Re}_x^{-1/2} = -2\frac{k_{hnf}}{k_f} c^{1/2}\theta'(c), \tag{11}$$

where $\mathrm{Re}_x = Ux/\nu_f$ is the Reynold number.

3. Methodology

The mathematical model was executed using the bvp4c function in MATLAB. The bvp4c method is highly effective in handling complex and robust problems, particularly for higher-order nonlinear boundary value problems. Many researchers have utilized this method to clarify and interpret solutions related to boundary value problems. The algorithm operates on an iterative framework, making it well-suited for solving systems of nonlinear equations. Additionally, bvp4c employs a finite difference formulation, utilizing the three-stage Lobatto IIIa method [22]. This approach provides a continuously driven solution that maintains uniform fourth-order accuracy over the interval $x \in [a, b]$.

As an iterative scheme, the bvp4c method requires careful selection of initial guesses for mesh points and appropriate step sizes to ensure convergence. To streamline the process, we developed two codes: code a, which handles the trial-and-error approach for the initial guess, and code b, which manages continuous iterations based on the initial guess. It is important to note that the nonlinear Eqs. (7) and (8), along with their boundary conditions (9), must first be reduced to a system of first-order ordinary differential equations. Let:

$$f = y(1), \quad f' = y(2), \quad f'' = y(3), \quad f''' = \frac{1}{\eta}\left[\frac{-y(1)y(3) + My(2)}{2\frac{\mu_{hnf}/\mu_f}{\rho_{hnf}/\rho_f}} - y(3)\right], \tag{12}$$

$$\theta = y(4), \quad \theta' = y(5), \quad \theta'' = \frac{1}{\eta}\left[\frac{-\Pr\, y(1)y(5)}{2\frac{k_{hnf}/k_f}{(\rho C_p)_{hnf}/(\rho C_p)_f}} - y(5)\right]. \tag{13}$$

The BCs in Eq. (9) become:

$$ya(1) = \frac{1}{2}\varepsilon c + 2\sigma c ya(3), \quad ya(2) = \frac{1}{2}\varepsilon + 2\sigma ya(3), \quad ya(5) = -\frac{k_f}{k_{hnf}}\mathrm{Bi}[1 - ya(4)],$$
$$yb(2) \to \frac{1-\varepsilon}{2}, \quad yb(4) \to 0. \tag{14}$$

The syntax of the solver sol = bvp4c (@OdeBVP, @OdeBC, solinit, options) includes commands for processing the function defined by @OdeBVP, as specified in Eqs. (12)–(13), along with the boundary conditions outlined in Eq. (14) that are handled by @OdeBC. The initial guess for the solution is represented by solinit. Furthermore, including the Odeinit argument in bvp4c allows for this initial guess, solinit, to also indicate the points at which the boundary conditions in @OdeBC are satisfied. The results obtained from the solver are presented as numerical solutions and graphs. Multiple solutions may exist for the problem when the approximate points of the initial guess also satisfy the boundary conditions. Further details can be found in the work of Shampine et al. [22]. It should be noted that the error tolerance of 10^{-6} is defined for the present case.

4. Results and discussion

The impact of the parameters will be investigated in relation to the results. The results are compared with values from a study by Ahmad et al. [4], Afridi et al. [5] and Aladdin et al. [8]. This comparison is done to ensure that the study is accurate and reliable. According to the study, the recent results are nearly identical, as shown in Table 2, thus confirming the accuracy of the figures found.

Table 2. Numerical comparison of $f''(c)$ when $\varepsilon = M = \sigma = \varphi_1 = \varphi_2 = 0$ for some values of c when $\Pr = 1$.

c	Ahmad et al. [4]	Afridi et al. [5]	Aladdin et al. [8]	Present	Error (%)
0.01	8.4924360	8.49233	8.4924366	8.492480326	0.00051488
0.1	1.2888171	1.28881	1.2888171	1.288778349	0.0030068
0.15			0.9383388	0.938431481	0.00987616
0.2			0.7515725	0.751664682	0.01226371

The results of different variations of flow parameters are presented and discussed as above. The parameters used for simulation are $c = 0.1$, $M = 0.1$, $\varphi_1 = \varphi_2 = 0.05$, $\varepsilon = -2$ and $\mathrm{Bi} = 0.01$, unless otherwise stated. Figures 2–7 show how velocity and temperature profiles change with different values c, M, φ_1, φ_2, σ, ε and Bi.

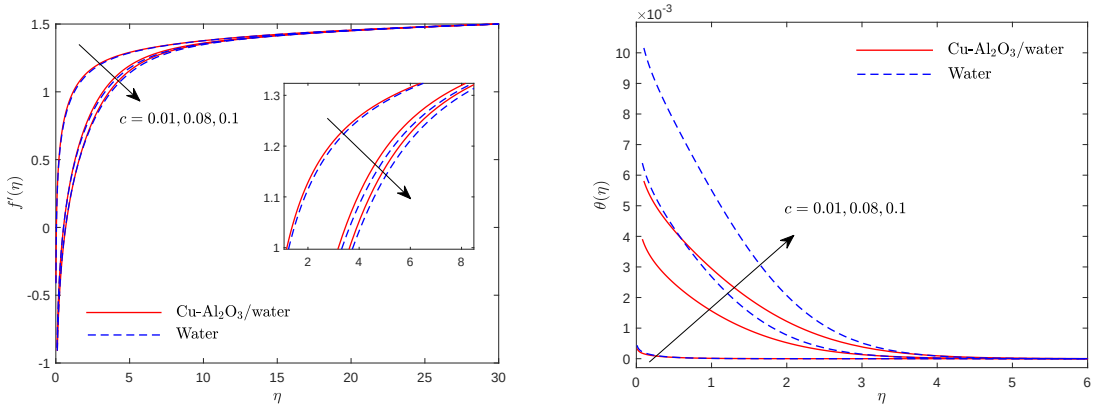

a ***b***

Fig. 2. Effects of c on (***a***) velocity profiles and (***b***) temperature profiles.

Figures 2a and 2b indicate how different needle size, c affect the velocity and temperature profiles. Figure 2a shows the velocity profile decreases as the parameter c increases. Additionally, the momentum boundary layer thickness also increases along with the increasing size of c. This is because, as the value of c decreases, the surface drag coefficient also decreases, which in turn increases the fluid velocity of both the Cu-Al_2O_3/water and water due to the altered physical conditions. It is also observed that a smaller needle size results in the less time required the heat and mass transfer the Cu-Al_2O_3/water and water to needle, thereby enhancing the rate of heat and mass transfer in the system. Additionally, the reduction in the momentum boundary layer thickness as c decreases enhance surface shear stress, thereby increasing the skin friction coefficient, as shown in Table 3. Figure 2b shows that both the temperature as well as the thermal boundary layer thickness increases as the size of the needle increases. A thinner needle size would result in the short amount of time for the heat to transfer between the needle and Cu-Al_2O_3/water and water. It can be proved by the decrement of the thermal boundary layer thickness as the size of the c decreases. The reduction in thermal boundary layer thickness resulted in a decreased rate of heat transfer, which decreases the Nusselt number as shown in Table 4. From Tables 3 and 4, it is shown that water has the lowest values of skin friction coefficient and heat transfer rate compared to Cu-Al_2O_3/water. Physically, suspending two types of nanoparticles into the base fluid increases surface friction. Notably, the presence of hybrid nanoparticles offers a larger surface area to volume ratio due to the high number of molecules at the boundaries. Therefore, this characteristic enhances Cu-Al_2O_3/water's stability in suspension, leading to improved thermal conductivity and an increased heat transfer rate compared to water.

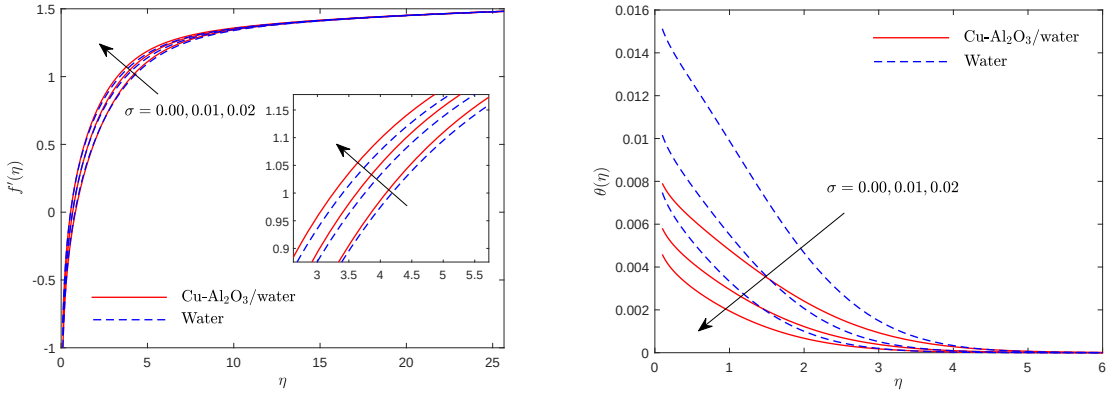

a ***b***

Fig. 3. Effects of σ on (***a***) velocity profiles and (***b***) temperature profiles.

The velocity profile in Figure 3a increases as the values for dimensionless slip length, increases while the momentum boundary layer thickness decreases. This occurs as the momentum boundary layer thicknesses significantly reduce as σ increases, reaching the ambient boundary condition more

quickly. In addition, the presence of slip also increases the skin friction coefficient for both water and hybrid nanofluid as shown in Table 3. Generally, incorporating a slip condition in the flow will reduce the drag along the wall which in turn enhances skin friction. It is observed that Cu-Al_2O_3/water has higher skin friction compared to water. Physically, the presence of hybrid nanofluid in the flow causes Cu-Al_2O_3/water to collide more frequently, enhancing the friction on the needle surface compared to water. On the other hand, Figure 3*b* illustrates the impact of different values of dimensionless slip length, σ on temperature profiles. It is shown that the temperature as well as the thermal boundary layer thickness decreases as σ increases. The reduction in the thermal boundary layer thickness leads to a lower Nusselt number as shown in Table 4.

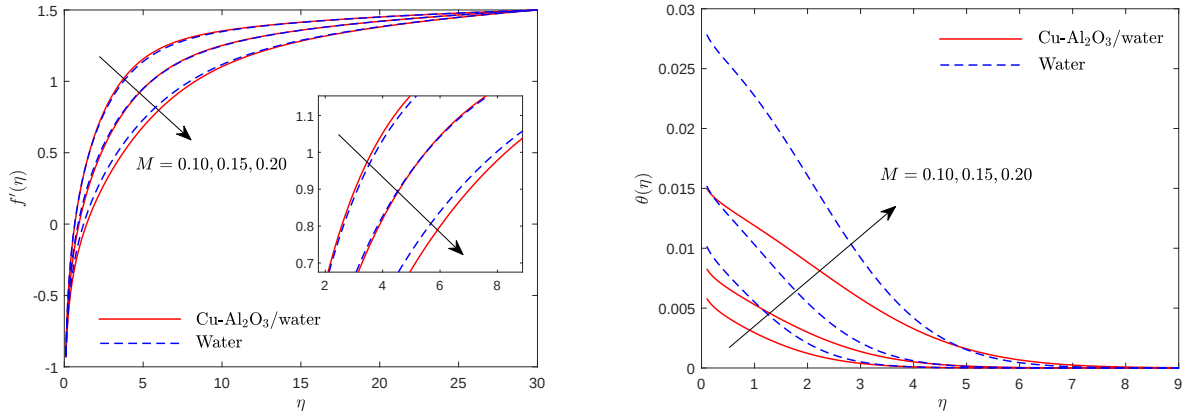

a ***b***

Fig. 4. Effects of M on (***a***) velocity profiles and (***b***) temperature profiles.

Figures 4*a* and 4*b* illustrate how the velocity and temperature profiles of a thin heated needle change with different values of the magnetic field parameter, M. Figures 4*a* and 4*b* highlights the influence of M on the velocity and temperatures profiles, respectively. As the value of M increases, the velocity profile decreases, while the momentum boundary layer thickness increases. This is because a stronger magnetic field as the value M increases, generates a Lorentz force that opposes the flow of fluid, thereby reducing the fluid velocity. Consequently, the momentum boundary layer becomes thicker. Magnetic fields can thus impact the flow characteristics of hybrid nanofluids because of this occurrence of a physical phenomenon which is the Lorentz force. As expected, the momentum boundary layer thickness for Cu-Al_2O_3/ water is greater than water. Figure 4*b* shows that as M increases, the temperature profile increases, which in addition leads to an increase in thermal boundary layer thickness. The skin friction and the Nusselt number decrease, as shown in Tables 3 and 4. It is evident that the skin friction and Nusselt number of Cu-Al_2O_3/ water is significantly lower than water (Tables 3 and 4).

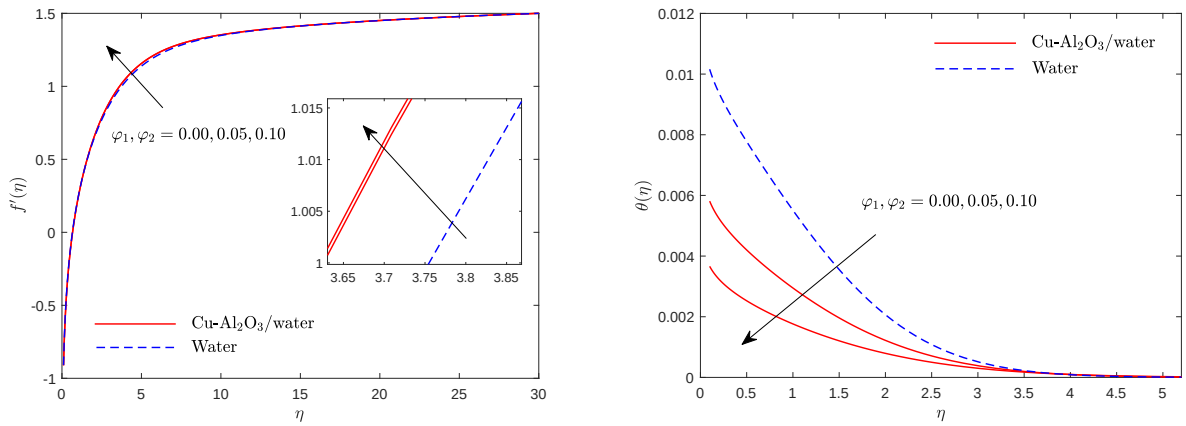

a ***b***

Fig. 5. Effects of φ_1 and φ_2 on (***a***) velocity profiles and (***b***) temperature profiles.

Figures 5a and 5b show the effects of changing the Cu and Al_2O_3 nanoparticles volume fraction, φ_1 and φ_2 for a moving vertical thin needle. When φ_1 and φ_2 increase, the velocity profile increases while the momentum boundary layer's thickness decreases respectively as shown in Figure 5a. This is because the collision of the two nanoparticles tends to enhance the drag force coefficient and thus increases the magnitude of the velocity profile. Based on Figure 5a it is observed that the velocity profile of hybrid nanofluid, Cu-Al_2O_3/water is higher than water. It is because when two different nanoparticles are combined, it will result in better performance for the velocity profile and thereby increases the skin friction as depicted in Table 3. Figure 5b illustrates that as the Cu and Al_2O_3 nanoparticles volume fraction, φ_1 and φ_2 increase, the temperature profile and thermal boundary layer thickness decreases accordingly. This occurs because, with more nanoparticles volume fraction, energy is dispersed more effectively and thus results in lower overall temperature profile across the hybrid nanofluid, Cu-Al_2O_3/water. Additionally, this is also due to the increment in the rate of heat transmission which then improves the value of the Nusselt number, as stated in Table 4.

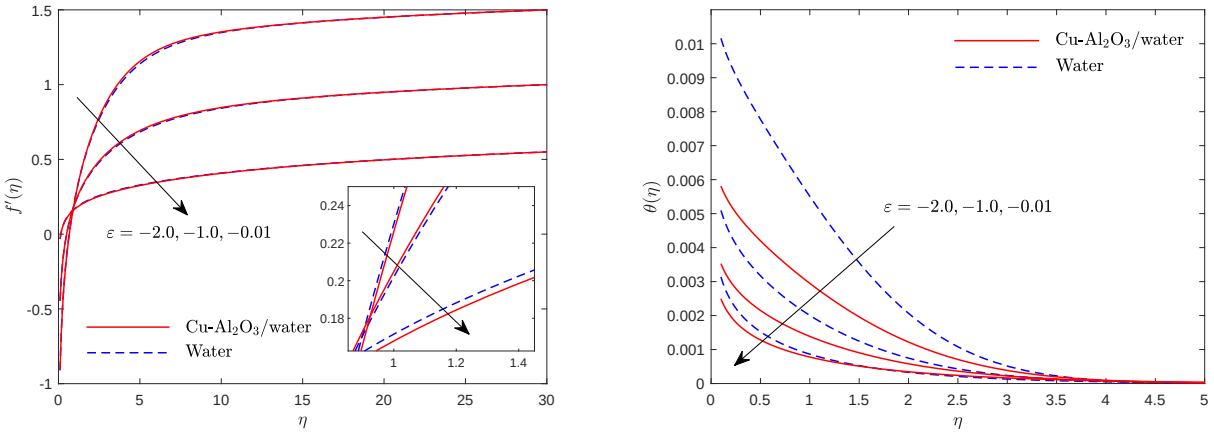

a ***b***

Fig. 6. Effects of ε on ($\boldsymbol{a}$) velocity profiles and ($\boldsymbol{b}$) temperature profiles.

Figures 6a and 6b shows the effects of changing the velocity ratio parameter, ε on a moving vertical thin needle. Based on Figure 6a, when the velocity ratio parameter, ε increases, the velocity profile decreases while the momentum boundary layer increases. This is because, when the velocity ratio parameter, ε increases, it will cause an increase in the resistance to the flow of hybrid nanofluid, Cu-Al_2O_3/water and water. Thus, this resistance will result in the declines of overall velocity profile due to restrained fluid movement. Furthermore, as the velocity ratio parameter, ε increases, the skin friction value, for both fluids decreases significantly as shown in Table 3. This happens due to a decrease in the free stream velocity. In addition, from Figure 6a and Table 3 it is observed that Cu-Al_2O_3/water has higher velocity profile and skin friction in comparison to water. Figure 6b indicates that when the velocity ratio parameter increases, ε the temperature profile and thermal boundary layer decrease. This occurs due to the efficient heat dissipation and thereby reduced the temperature profile near the surface of the needle. In Table 4, the enhanced convective heat transfer effectively increases the Nusselt number Cu-Al_2O_3/water of compared to water.

Figures 7a and 7b shows the velocity profile and temperature profile of Cu-Al_2O_3/water and water when the value of Bi increases. Based on Figure 7a, the velocity profile of Cu-Al_2O_3/water and water remain unchanged when the Bi increases. On the other hand, Figure 7b illustrates that the temperature profile and thermal boundary layer thickness for both Cu-Al_2O_3/water and water increase as the Bi increases. This happens because higher amount of Bi improves the rate of heat transfer. Additionally, this will lead to efficient convective heat transfer which then significantly improves the Nusselt number as shown in Table 4. Furthermore, it is also observed that Cu-Al_2O_3/water has higher Nusselt numbers in comparison to water as the value of Bi grows. This is due to the presence of nanoparticles in Cu-Al_2O_3/water which leads to the enhancement of thermal conductivity.

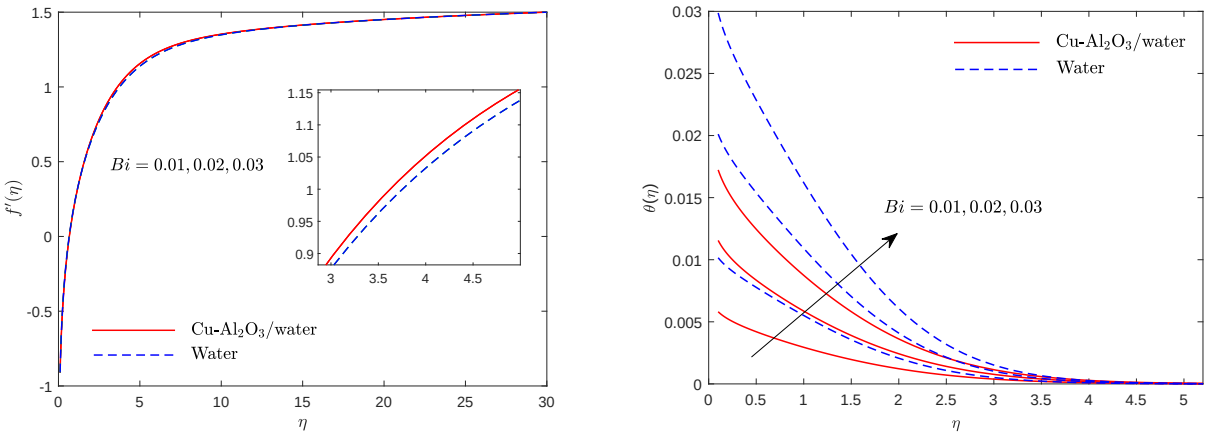

a ***b***

Fig. 7. Effects of Bi on (***a***) velocity profiles and (***b***) temperature profiles.

Table 3. Variation of the skin friction coefficient at different dimensionless parameters for Cu-Al_2O_3/water and water.

c	M	φ_1	φ_2	σ	ε	Bi	Water	Cu-Al_2O_3/water
0.01							11.755755	15.342067
0.08	0.1	0.05	0.05	0.01	-2	0.01	6.365126	8.149592
0.10							5.727790	7.262329
	0.1						5.727790	7.262329
0.1	0.15	0.05	0.05	0.01	-2	0.01	4.995484	6.188468
	0.2						4.339563	5.202135
		0	0				5.727790	
0.1	0.1	0.05	0.05	0.01	-2	0.01		7.262329
		0.1	0.1					9.507601
				0			5.590805	6.982728
0.1	0.1	0.05	0.05	0.01	-2	0.01	5.727790	7.262329
				0.02			5.793464	7.423625
					-2		5.727790	7.262329
0.1	0.1	0.05	0.05	0.01	-1	0.01	3.426186	4.417021
					-0.1		1.110696	1.409615
						0.01	5.727790	7.262329
0.1	0.1	0.05	0.05	0.01	-2	0.02	5.727790	7.262329
						0.03	5.727790	7.262329

Table 4. Variation of Nusselt number at different dimensionless parameters for Cu-Al_2O_3/water and water.

c	M	φ_1	φ_2	σ	ε	Bi	Water	Cu-Al_2O_3/water
0.01							0.001999	0.001999
0.08	0.1	0.05	0.05	0.01	-2	0.01	0.005620	0.005634
0.10							0.006260	0.006287
	0.1						0.006260	0.006287
0.1	0.15	0.05	0.05	0.01	-2	0.01	0.006228	0.006272
	0.2						0.006148	0.006229
		0	0				0.006260	
0.1	0.1	0.05	0.05	0.01	-2	0.01		0.006287
		0.1	0.1					0.006301
				0			0.006228	0.006274
0.1	0.1	0.05	0.05	0.01	-2	0.01	0.006260	0.006287
				0.02			0.006277	0.006295
					-2		0.006260	0.006287
0.1	0.1	0.05	0.05	0.01	-1	0.01	0.006292	0.006302
					-0.1		0.006304	0.006308
						0.01	0.006260	0.006287
0.1	0.1	0.05	0.05	0.01	-2	0.02	0.012394	0.012502
						0.03	0.018406	0.018646

5. Conclusion

The study examined boundary layer flow past a heated needle in hybrid nanofluid. The nonlinear PDEs were transformed into dimensionless ODEs using similarity transformation and solved numerically with MATLAB's bvp4c solver. It was observed that various governing parameters influenced the velocity and temperature profiles, with the velocity profile affecting skin friction and the temperature profile impacting the local Nusselt number. The study made comparisons between hybrid nanofluid, Cu-Al_2O_3, and the base fluid, water, focusing on skin friction coefficient and heat transfer rate. The outcome of this study are as follows:

1. The velocity profiles decrease with increasing values of c, M and ε, while they increase with higher values of σ, as well as the nanoparticles, φ_1 and φ_2. The velocity profiles remain constant for Bi.
2. The temperature profiles increase with higher values of c, M and Bi, while they decrease with increasing values of φ_1, φ_2, σ and ε.
3. The skin friction values increase as the value for φ_1, φ_2 and σ increases, while decreases as the value for c, M and ε. The skin friction for Bi remains constant as the parameter increases.
4. The Nusselt number values increase with rising values of c, φ_1, φ_2, σ, ε and Bi, except for M.
5. The hybrid nanofluid, Cu-Al_2O_3, exhibits higher values of skin friction and Nusselt number than water across all parameters. The findings demonstrate that the hybrid nanofluid significantly enhances both the skin friction coefficient and heat transfer rate compared to the base fluid.

Acknowledgement

This work was funded by Ph.D. Graduate MyRA Research Grant (600-RMC/GPM LPHD 5/3 (158/2021)) from Universiti Teknologi MARA.

[1] Choi S. U. S., Eastman J. A. Enhancing thermal conductivity of fluids with nanoparticles. Argonne National Lab. (ANL), Argonne, IL, United States (1995).

[2] Eastman J. A., Choi U. S., Li S., Thompson L. J., Lee S. Enhanced thermal conductivity through the development of nanofluids. MRS Online Proceedings Library. **457**, 3–11 (1996).

[3] Yildiz Ç., Arici M., Karabay H. Comparison of a theoretical and experimental thermal conductivity model on the heat transfer performance of Al_2O_3-SiO_2/water hybrid-nanofluid. International Journal of Heat and Mass Transfer. **140**, 598–605 (2019).

[4] Ahmad S., Arifin N. M., Nazar R., Pop I. Mixed convection boundary layer flow along vertical thin needles: Assisting and opposing flows. International Communications in Heat and Mass Transfer. **35** (2), 157–162 (2008).

[5] Afridi M. I., Tlili I., Goodarzi M., Osman M., Khan N. A. Irreversibility analysis of hybrid nanofluid flow over a thin needle with effects of energy dissipation. Symmetry. **11** (5), 663 (2019).

[6] Waini I., Ishak A., Pop I. Hybrid nanofluid flow and heat transfer past a vertical thin needle with prescribed surface heat flux. International Journal of Numerical Methods for Heat & Fluid Flow. **29** (12), 4875–4894 (2019).

[7] Hamid A. Terrific effects of Ohmic-viscous dissipation on Casson nanofluid flow over a vertical thin needle: buoyancy assisting & opposing flow. Journal of Materials Research and Technology. **9** (5), 11220–11230 (2020).

[8] Aladdin N. A. L., Bachok N., Pop I. Boundary layer flow and heat transfer of Cu-Al_2O_3/water over a moving horizontal slender needle in presence of hydromagnetic and slip effects. International Communications in Heat and Mass Transfer. **123**, 105213 (2021).

[9] Prashar P., Ojjela O., Kambhatla P. K., Das S. K. Numerical investigation of boundary layer flow past a thin heated needle immersed in hybrid nanofluid. Indian Journal of Physics. **96**, 137–150 (2022).

[10] Singh P., Kumar D., Kumari A. Effect of heat and mass transfer in nanofluid flow along a vertical thin needle. Materials Today: Proceedings. **57**, 2276–2280 (2022).

[11] Ali B., Jubair S., Al-Essa L. A., Mahmood Z., Al-Bossly A., Alduais F. S. Boundary layer and heat transfer analysis of mixed convective nanofluid flow capturing the aspects of nanoparticles over a needle. Materials Today Communications. **35**, 106253 (2023).

[12] Waini I., Ishak A., Pop I. Hybrid nanofluid flow and heat transfer past a permeable stretching/shrinking surface with a convective boundary condition. Journal of Physics: Conference Series. **1366**, 012022 (2019).

[13] Sajid T., Al Mesfer M. K., Jamshed W., Eid M. R., Danish M., Irshad K., Ibrahim R. W., Batool S., El Din S. M., Altamirano G. C. Endo/exothermic chemical processes influences of tri-hybridity nanofluids flowing over wedge with convective boundary constraints and activation energy. Results in Physics. **51**, 106676 (2023).

[14] Jan S. U., Khan U., El-Rahman M. A., Islam S., Hassan A. M., Ullah A. Effect of variable thermal conductivity of ternary hybrid nanofluids over a stretching sheet with convective boundary conditions and magnetic field. Results in Engineering. **20**, 101531 (2023).

[15] Jusoh R., Naganthran K., Jamaludin A., Ariff M. H., Basir M. F. M., Pop I. Mathematical analysis of the flow and heat transfer of Ag-Cu hybrid nanofluid over a stretching/shrinking surface with convective boundary condition and viscous dissipation. Data Analytics and Applied Mathematics. **1** (1), 11–22 (2020).

[16] Ilias M. R., Ismail N. S., Ab Raji N. H., Rawi N. A., Shafie S. Unsteady aligned MHD boundary layer flow and heat transfer of a magnetic nanofluids past an inclined plate. International Journal of Mechanical Engineering and Robotics Research. **9**, 197–206 (2020).

[17] Song Y.-Q., Hamid A., Khan M. I., Gowda R. J. P., Kumar R. N., Prasannakumara B. C., Khan S. U., Khan M. I., Malik M. Y. Solar energy aspects of gyrotactic mixed bioconvection flow of nanofluid past a vertical thin moving needle influenced by variable Prandtl number. Chaos, Solitons & Fractals. **151**, 111244 (2021).

[18] Sulochana C., Samrat S. P., Sandeep N. Boundary layer analysis of an incessant moving needle in MHD radiative nanofluid with joule heating. International Journal of Mechanical Sciences. **128–129**, 326–331 (2017).

[19] Souayeh B., Reddy M. G., Sreenivasulu P., Poornima T., Rahimi-Gorji M., Alarifi I. M. Comparative analysis on non-linear radiative heat transfer on MHD Casson nanofluid past a thin needle. Journal of Molecular Liquids. **284**, 163–174 (2019).

[20] Devi S. P. A., Devi S. S. U. Numerical investigation of hydromagnetic hybrid Cu-Al_2O_3/water nanofluid flow over a permeable stretching sheet with suction. International Journal of Nonlinear Sciences and Numerical Simulation. **17**, 249–257 (2016).

[21] Oztop H. F., Abu-Nada B. Numerical study of natural convection in partially heated rectangular enclosures filled with nanofluids. International Journal of Heat and Fluid Flow. **29** (5), 1326–1336 (2008).

[22] Shampine L. F., Gladwell I., Thompson S. Solving ODEs with MATLAB. Cambridge University Press (2003).

Магнітогідродинамічний потік гібридної нанорідини над нагрітою тонкою голкою

Іліас М. Р.[1,3], Аванг Н.[2], Фазрі Н. Н.[2], Росмаді С. А. А.[2], Саллех С. Н. А.[4], Назар Р. М.[3]

[1] *Школа обчислювальної техніки, інформатики та математики, Університет технологій MARA, 40450 Шах Алам, Селангор, Малайзія*

[2] *Вивчення математичних наук, Коледж обчислювальної техніки, інформатики та математики, Філія технологічного університету MARA у Негері Сембілані, кампус Серембан, 70300 Серембан, Негері Сембілан, Малайзія*

[3] *Кафедра математичних наук, факультет науки і технологій, Національний університет Малайзії, Бангі 43600, Малайзія*

[4] *Вивчення математичних наук, Коледж обчислювальної техніки, інформатики та математики, Філія технологічного університету MARA в Кедахі, 08400 Мербок, Кедах, Малайзія*

Суспендування наночастинок в базовій рідині може ефективно покращити теплопровідність рідини. Тому дослідження зосереджено на постійному двовимірному ламінарному потоці граничного шару з примусовою конвекцією вздовж горизонтальної тонкої нагрітої голки, яка занурена в гібридну нанорідину з конвективною граничною умовою. Для цього дослідження були обрані наночастинки оксиду міді та алюмінію з водою як основною рідиною. Основні диференціальні рівняння в частинних похідних перетворюються на нелінійні звичайні диференціальні рівняння за допомогою відповідного перетворення подібності. Потім ці рівняння розв'язуються чисельно за допомогою пакета bvp4c у програмному забезпеченні MATLAB. Вплив залучених параметрів, включаючи об'ємну частку наночастинок, товщину голки, співвідношення швидкостей, безрозмірну довжину ковзання, взаємодію магнітного поля та конвективних граничних умов на профілі швидкості та температури, а також коефіцієнт поверхневого тертя та локальне число Нуссельта, проілюстровано за допомогою графіків і таблиць. Результат показує, що зі збільшенням об'ємної частки наночастинок і параметра безрозмірної довжини ковзання профіль швидкості збільшується. З іншого боку, температура підвищується зі збільшенням параметрів товщини голки, безрозмірної довжини ковзання, взаємодії магнітного поля, об'ємної частки наночастинок, параметра співвідношення швидкостей і конвективної граничної умови. Загалом, зі збільшенням параметрів Cu-Al_2O_3/вода має вищі значення поверхневого тертя та числа Нуссельта порівняно з водою. Застосування цього дослідження можна застосувати в галузі біомедичної інженерії, де нагріті голки відіграють вирішальну роль у медичних процедурах, таких як термічна абляція, доставка ліків і мінімально інвазивні операції.

Ключові слова: *гібридна нанофлюїд; горизонтальна тонка голка; магнітогідродинаміка; конвективна гранична умова.*